Dynamical scaling properties of nanoporous undoped and Sb-doped SnO_2 supported thin films during tri- and bidimensional structure coarsening

C. V. Santilli,* A. P. Rizzato, and S. H. Pulcinelli
Instituto de Química/UNESP, P.O. Box 355, Araraquara, São Paulo 14800-900, Brazil

A. F. Craievich
Instituto de Física/USP, P.O. Box 66318, São Paulo, São Paulo 05315-970, Brazil
(Received 17 January 2007; published 23 May 2007)

The coarsening of the nanoporous structure developed in undoped and 3% Sb-doped SnO_2 sol-gel dip-coated films deposited on a mica substrate was studied by time-resolved small-angle x-ray scattering (SAXS) during *in situ* isothermal treatments at 450 and 650 °C. The time dependence of the structure function derived from the experimental SAXS data is in reasonable agreement with the predictions of the statistical theory of dynamical scaling, thus suggesting that the coarsening process in the studied nanoporous structures exhibits dynamical self-similar properties. The kinetic exponents of the power time dependence of the characteristic scaling length of undoped SnO_2 and 3% Sb-doped SnO_2 films are similar ($\alpha \approx 0.09$), this value being invariant with respect to the firing temperature. In the case of undoped SnO_2 films, another kinetic exponent, α', corresponding to the maximum of the structure function was determined to be approximately equal to three times the value of the exponent α, as expected for the random tridimensional coarsening process in the dynamical scaling regime. Instead, for 3% Sb-doped SnO_2 films fired at 650 °C, we have determined that $\alpha' \approx 2\alpha$, thus suggesting a bidimensional coarsening of the porous structure. The analyses of the dynamical scaling functions and their asymptotic behavior at high q (q being the modulus of the scattering vector) provided additional evidence for the two-dimensional features of the pore structure of 3% Sb-doped SnO_2 films. The presented experimental results support the hypotheses of the validity of the dynamic scaling concept to describe the coarsening process in anisotropic nanoporous systems.

DOI: 10.1103/PhysRevB.75.205335 PACS number(s): 68.55.−a, 61.10.Eq, 61.43.Gt

I. INTRODUCTION

Antimony-doped tin oxide (ATO) thin films are of widespread interest because of their high electrical conductivity, optical transparency in the visible wavelengths range, chemical and thermal stability, good adhesion to glass substrate, scratch resistance, and easy patterning ability.[1] These properties make ATO thin films useful for many applications such as protective layers for glasses, transparent electrodes in various display devices and solar cells, antistatic coatings, selective semiconductor gas sensors, and heating elements for mirrors and glass windows.[2–6] To satisfy the requirements of this wide field of applications, growing efforts have been made on the preparation of ATO films by using the sol-gel process.[5–14] This process has the advantages of making possible (i) coatings on large areas with an easy control of the doping level and (ii) achieving a good homogeneity without using expensive and complex equipment when compared with other film deposition techniques.

The SnO_2 films obtained by sol-gel route are built of nearly spherical loosely packed nanocrystalline particles, thereby offering a large specific area and large density of grain boundaries. Such accessible internal nanoporosity is desirable for surface reactions of adsorbed species, thus improving the sensitivity of the SnO_2-based gas sensor,[4] and allows for the creation of a microelectrochemical reactor chamber for specific electrocatalytic transformations, while the transparency of the final material provides the opportunity for tunable optical display devices.[5,14] Because of this nanosized nature of the pore structure, the lowest value of the resistivity of sol-gel derived ATO films exceeds by more than 1 order of magnitude those obtained by other deposition methods.[6–12]

There are many experimental evidences indicating that the addition of group V elements, that are used as electron donor doping in order to increase the conductivity of SnO_2-based materials, affects also the film nanostructure and its stability upon firing.[8–12] In the specific case of ATO films and powdered xerogels, the increase of doping level causes a decrease in average crystallite size and an increase in nanoporosity volume.[11,12] The reasons for which the Sb doping inhibits the crystallite growth are still not clear. Some authors[12] suggested that the Sb doping plays a role similar to that reported for Nb_2O_5- and CuO-doped SnO_2,[15–17] in which an enrichment of cations on the surface of the crystallites upon firing occurs, thus restricting the crystallite growth. Another previous article[18] about the preparation of ATO films using an Sb^{III} source reported a drop of several orders of magnitude (about seven) of their resistivity after firing at around 500 °C. At this temperature, the oxidation of Sb^{III} to Sb^{V} and the incorporation of antimony into cassiterite structure occur. Thus, the improvement of conductivity and the control of crystallite growth induced by Sb doping were explained by the coexistence of Sb^{V} incorporated into the host cassiterite structure and of Sb^{III} segregated at the particle surface.[18]

Since the nanostructural features and doping distribution are of paramount importance for the electronic properties of ATO films, these materials have been investigated by several methods including x-ray-absorption fine-structure,[18]

photoelectron,[19,20] Mössbauer,[21] and infrared[22] spectroscopies. Despite these efforts, the effect of Sb doping on the porosity evolution and nanocrystallite growth upon isothermal treatment of ATO films is still not well understood. The goal of this paper is to analyze the time evolution of the porous nanostructure of both undoped and Sb-doped SnO_2 films during isothermal treatments at different temperatures.

As already done for undoped xerogel[23] and copper-doped SnO_2 unsupported thick films,[16] small-angle x-ray scattering (SAXS) techniques were used to study *in situ* the kinetics of densification and nanoporosity coarsening in supported ATO films. The dynamical scaling and other statistical properties of the structure function determined from SAXS results were applied to analyze the pore growth process of undoped and Sb-doped samples.

II. BASIC THEORY

Nanoporous SnO_2 powders and unsupported thick films prepared by dip coating and maintained at constant temperature between 400 and 700 °C do not exhibit any significant macroscopic densification effect. For isotropic systems satisfying this condition, the time evolution of the porous structure is governed only by coarsening effects. These effects can be described by a statistical theory that predicts dynamical scaling properties for the structure function of the system.[16,23] This theory was firstly applied to describe the coarsening process that occurs during the advanced stage of phase separation in binary crystalline alloys and amorphous oxide mixtures, when both phases have reached the equilibrium compositions and their volume fractions become time invariant.[24–26] In these systems, the coarsening process evolves through a dynamical self-similar mode, i.e., the structural variation being described as a dynamical and uniform magnification with a single characteristic length.

The structure function $S(q)$ is the Fourier transform of the spatial correlation function of isotropic structures in real space. A time-dependent structure function $S(q,t)$ is often used to describe the structural variations during nanophase separation processes. The structure function $S(q,t)$ is equivalent to the SAXS intensity $I(q,t)$ provided this function is properly normalized. The modulus of the scattering vector is defined in SAXS experiments as $q=(4\pi/\lambda)\sin\theta$, θ being half the scattering angle and λ the x-ray wavelength. Statistical theories applied to isotropic binary systems in advanced stages of phase separation predict that $I(q,t)$ and $S(q,t)$ both exhibit a scaling property that depends on a single characteristic length $R(t)$ as specified in the following equation:[24–26]

$$I(q,t) = S(q,t) = [R(t)]^d F(x), \tag{1}$$

where d is the dimensionality of the system, $F(x)$ is a time-independent scaling function, and x is defined as $x=q/q_1$, where q_1 is the first normalized moment of the structure function.

The scaling function $F(x)$ exhibits a maximum for $x \cong 1$ and a simple asymptotic dependence on the modulus of the scattering vector over the high-q range ($q > q_1$). In the case of a two-phase system with a smooth and thin interface as compared to the phase dimensions, the asymptotic behavior of $F(x)$ obeys the Porod law:[27,28]

$$F(x) \propto x^p = x^{-(d+1)}, \quad x \gg 1. \tag{2}$$

An exponent $p=-(d+1)$ lower than -4 (for $d=3$) is expected when the interface is not sharp, i.e., when the electronic density, instead of having a steep discontinuity, exhibits a smooth variation between their values corresponding to each phase. In fact, the effect of the interfacial structure on the Porod tail can be observed only for large wave numbers ($x>2$).[28] For intermediate wave number ($1<x<2$) the tail of $F(x)$ can be approximated by the same equation [Eq. (2)] with characteristic p values. Consequently, the scaling functions exhibit a crossover from x^p (for $1<x<2$) to x^{-4} ($x>2$). When the volume fraction of the minority phase exceeds the percolation threshold, a bicontinuous pattern with a wavy or tangled interface is expected. In this case, the scaling functions at intermediate wave number ($1<x<2$) are expected to display a tail described by Eq. (2) for which the exponent $p=-2d$.[28]

In order to test the validity of the dynamical scaling properties of the structure function, we can analyze the time dependences of the moments $S_n(t)$ and normalized moments $q_n(t)$ of the structure function, defined as follows:

$$S_n(t) = \int_0^\infty I(q,t) q^n dq, \quad n = 0,1,2, \ldots, \tag{3}$$

and

$$q_n(t) = \frac{S_n(t)}{S_0(t)}, \quad n = 1,2, \ldots. \tag{4}$$

The moment $S_n(t)$ and the normalized first moment $q_1(t)$ of the structure functions are related by

$$S_n(t) = K_n[q_1(t)]^{n-2}, \quad n = 0,1,2, \tag{5}$$

where $K_n(t)=\int_0^\infty x^n F(x)dx$.

Because of the invariance of the total volume fraction of both phases, the theory of dynamical scaling predicts that the following quantities are time independent:

$$S_2 = C_1, \quad S_o/S_1^2 = C_2, \quad S_m q_1^3 = C_3, \quad \text{and } q_2/q_1^2 = C_4. \tag{6}$$

The characteristic length is defined as the reciprocal value of the normalized first moment $R(t)=1/q_1$. Thus, it is expected that $q_1(t)$ and the maximum intensity of the SAXS curve, $I_m(t)$, evolve with time according to[28]

$$q_1(t) \propto t^{-\alpha} \tag{7}$$

and

$$I_m(t) \propto t^{\alpha'} \text{ or } I_m(t) \propto q_1^d, \tag{8}$$

where

$$d = \alpha'/\alpha. \tag{9}$$

The exponent α depends on the dominant coarsening mechanism, and d is the dimensionality of the coarsening

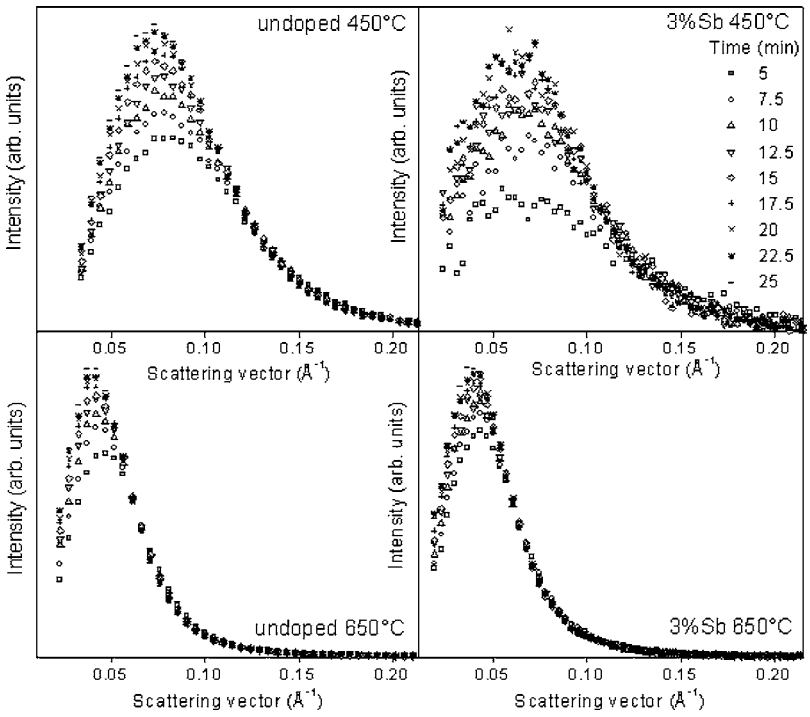

FIG. 1. Sets of SAXS curves $[I(q)$ vs $q]$ corresponding to undoped SnO_2 and 3% Sb-doped SnO_2 supported films maintained during different time periods at 450 and 650 °C.

process. The experimental verifications of Eqs. (6)–(9) are often used as tests of validity for the hypothesis under which the dynamical scaling theory applies. Furthermore, the ratio α'/α yields the dimensionality d of the coarsening process.[28]

III. EXPERIMENTAL PROCEDURES

A. Sample preparation

Transparent and stable, both undoped and 3% by weight Sb-doped, SnO_2 colloidal suspensions were prepared by hydrolysis of $SnCl_4 \cdot 5H_2O$ in aqueous solution using a previously described procedure.[29] These colloidal suspensions were used as precursor for the deposition of SnO_2 and ATO films on mica substrate by the dip-coating process with withdrawal speed of 8 cm/min. In order to obtain films thick enough for SAXS measurements, the dip-coating procedure was repeated 20 times. After drying for 10 min at 25 °C and 30 min at 110 °C, ≈200 nm thick films were obtained.

B. SAXS measurements

SAXS measurements were performed using the SAXS beamline at the National Synchrotron Light Laboratory (LNLS), Campinas, Brazil. This beamline is equipped with an asymmetrically cut and bent silicon (111) monochromator producing a monochromatic ($\lambda = 1.608$ Å) and horizontally focused beam. Because of the small size of the incident-beam cross-section at the detection plane, no mathematical desmearing of the experimental SAXS function was needed. A position-sensitive linear detector and a multichannel analyzer were used to record the SAXS intensity $I(q)$ as a function of the modulus of the scattering vector q.

The parasitic scattering from slits and air was subtracted from the total scattering intensity. The resulting curves were normalized to account for the effects related to the natural decay in intensity of the synchrotron source, detector sensitivity, and sample transmission and thickness. SAXS data collection started just after placing the sample into the furnace maintained at constant temperature ($T = 450$ and 650 °C). Each spectrum was recorded *in situ* during a time interval of 150 s.

IV. RESULTS

The time evolution of SAXS curves measured *in situ* during isothermal firing at 450 and 650 °C for undoped and Sb-doped films are plotted in Fig. 1. The observed SAXS intensity was associated with the nanoporous structure of the studied materials, which can be considered essentially as a two-phase system consisting of a solid matrix and pores. All spectra exhibit a characteristic wide peak attributed to the existence of spatial pore-pore, matter-matter, and pore-matter correlations.[16,23] The q position and the maximum of the SAXS peak, that is observed in all SAXS curves (Fig. 1), vary with time and depend both on the temperature of isothermal treatment and on the addition of Sb doping.

For all, undoped and doped, samples heat treated at 450 and 650 °C, the maximum of the peak I_m increases with time, while its coordinate q_m decreases, thus indicating the existence of an overall coarsening of the nanoporous structure. Qualitatively, this is an expected feature for an evolving two-phase system that exhibits the dynamical scaling property of the structure function, as described by Eq. (1).[24–28] A necessary condition for the validity of the dynamical scaling property is that the evolving two-phase system maintains time-independent electron density contrast and volume fractions of both phases.

The validity of the statistical properties described in Sec. II for the porous system studied here was verified by analyz-

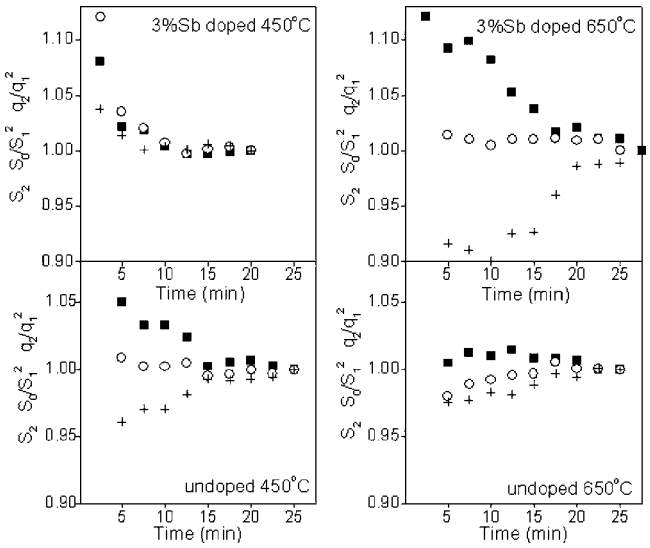

FIG. 2. Time dependences of (■) $S_2(t)/S_2(t_f)$, (+) $[(S_0(t))/(S_1^2(t))]/[(S_0(t_f))/S_1^2(t_f)]$, and (○) $[q_2(t)/q_1^2(t)]/[q_2(t_f)/q_1^2(t_f)]$ for undoped and 3% Sb-doped supported SnO_2 films fired at 450 and 650 °C.

ing the different sets of experimental SAXS curves during the coarsening process. The different moments S_0, S_1, and S_2 of the structure function were calculated from the experimental $I(q,t)$ function by integrating numerically $I(q)$, $I(q)q$, and $I(q)q^2$, respectively, within the range $0.02<q<0.35$ Å^{-1}. The part of the integrals corresponding to $q>0.35$ Å^{-1} was determined using the SAXS intensity derived from the Porod law and, for $q<0.02$ Å^{-1}, by linear extrapolation from $q=0.02$ Å^{-1} to $q=0$, assuming $I(0)=0$.

V. DISCUSSION

A. Statistical properties of the structure function

An experimental procedure that is often applied to test the hypothesis underlining the dynamical scaling properties is to investigate the time variations of the moments and quotient between moments of the structure function as those predicted by Eqs. (5) and (6). Particularly, as mentioned in Sec. II, the quantities $S_2(t)$, $S_0(t)/S_1^2(t)$, and $q_2(t)/q_1^2(t)$ are expected to be time invariant for advanced stages of firing.

The different quotients $S_2(t)/S_2(t_f)$, $[(S_0(t))/(S_1^2(t))]/[(S_0(t_f))/S_1^2(t_f)]$, and $[q_2(t)/q_1^2(t)]/[q_2(t_f)/q_1^2(t_f)]$ are displayed as functions of time in Fig. 2, where t_f is the longest time of firing at each temperature. These functions are expected to be invariant and equal to 1 during the final stages of the structural evolution, when the total volume of pores remains constant (i.e., during the coarsening stage). Our results corresponding to different temperatures exhibit the following common features:

(i) All quantities mentioned above vary with time for undoped and Sb-doped samples fired at 450 °C during the first 10–15 min. In particular, the decrease of the second moment S_2 indicates that the total volume of pores decreases with time during the early period of isothermal treatment. This feature is a consequence of the secondary condensation reaction involving OH groups present at the particle surfaces and boundaries, which takes place during heating between 250 and 450 °C. As a consequence of this dehydration reaction, the interparticle distance, the film thickness, and the volume fraction of pores decrease.[11]

(ii) For undoped samples fired at 650 °C, all statistical parameters displayed in Fig. 2 are essentially time invariant during the whole firing period, thus demonstrating the general validity of Eqs. (5) and (6). Furthermore, these features indicate that the mentioned dehydration processes (observed for samples heat treated at 450 °C) are very fast at 650 °C, so they were not recorded in our time-resolved experiments performed at this temperature.

(iii) For 3% Sb-doped films, the regime of time invariance expected for the second moment $S_2(t)$ and for the ratio $S_0(t)/S_1^2(t)$ is reached only at very advanced periods of firing at 650 °C. On the contrary, q_2/q_1^2 attains an essentially constant value relatively early at this temperature. In fact, these moments are related by the total integrated intensity S_2 by

$$\frac{S_0}{S_1^2}=\left(\frac{1}{S_2}\right)\frac{q_2}{q_1^2}. \tag{10}$$

Thus, the invariance of q_2/q_1^2 observed in Fig. 2 indicates that the variation of S_2 is responsible for the deviation of the $S_0(t)/S_1^2(t)$ from the behavior theoretically predicted by the scaling relation [Eq. (5)]. The main causes of these features are discussed below.

For 3% Sb-doped films fired at 650 °C, the explanation of the time variation of S_2 as being induced by the change in total pore volume can be discarded because the mentioned effects produced by dehydration at this temperature are too fast to be observed in our time resolved SAXS experiments. Furthermore, it is known that the overall densification of SnO_2-based ceramic only occurs for firing at temperatures higher than 1200 °C and that anisotropic processes of crystallite growth and nanopore coarsening can occur at lower temperature.[11,30] Thus, we have concluded that the deviation from the theoretical behavior observed for quantities S_2 and $S_0(t)/S_1^2(t)$ is associated with intrinsic features related to a non-three-dimensional growth process of nanopores present at SnO_2 crystallites boundaries.

As previously mentioned, the dimensionality of the space in which the coarsening process occurs during the dynamical scaling regime can be determined from the experimental SAXS results either from the quotient $d=\alpha'/\alpha$ or as the slope of the straight line in the log-log plots of $I_m(t)$ vs $q_1(t)$ [Eq. (8)]. These plots corresponding to undoped and Sb-doped films during firing at 450 and 650 °C are displayed in Fig. 3 in double-logarithmic scale. The linear behavior of $\log I_m$ versus $\log q_1$ plots, predicted by Eq. (9), is obeyed for all composition and temperature conditions along the whole process, thus indicating that the dimensionality of the coarsening process is invariant during the whole time period of isothermal firing.

Table I lists the values of $d=(\alpha'/\alpha)$ derived from the slopes determined by linear least-squares fitting of the experimental points (dashed lines in Fig. 3). For undoped SnO_2 films fired at 450 and at 650 °C, we have determined a di-

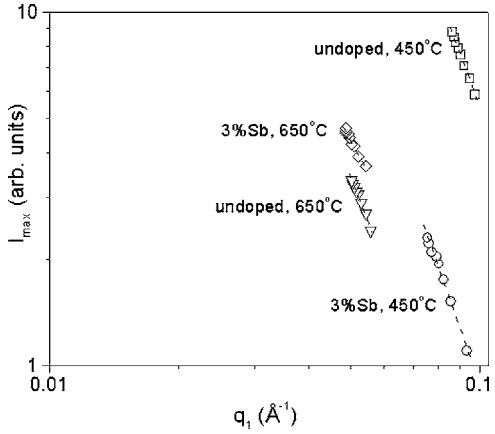

FIG. 3. Double-logarithmic plot of the maximum of SAXS intensity I_{max} as a function of the first normalized moment q_1 corresponding to undoped and Sb-doped films fired at 450 and 650 °C. The different slopes of the straight lines corresponding to the exponent ratios $\alpha'/\alpha=d$ are given in Table I.

mensionality $d=3$, this value being expected from the scaling property for isotropic systems that evolves through a tridimensional coarsening process. The similar values of the (α'/α) ratios for both undoped and Sb-doped SnO_2 samples fired at 450 °C ($\alpha'/\alpha \approx 3$) indicate that the coarsening process occurs in three dimensions for both samples. Instead, the clearly different values of the (α'/α) ratios for undoped and doped samples fired at 650 °C ($\alpha'/\alpha \approx 3$ and 2, respectively) confirm the strong effect of Sb doping in the dimensionality of the structure coarsening process, which occurs in two dimensions at this temperature

Taking into account the clearly bidimensional nature of the coarsening process for 3% Sb-doped samples fired at 650 °C, we propose that the variation of S_2—while q_2/q_1^2 remains essentially invariant—is not a consequence of changes in the total pore volume, as in the case of the same samples fired at 450 °C. Instead, we have assigned this variation to the bidimensional nature of the coarsening process in the nanoporous structure.

The bidimensional nature of the porous structure for the 3% Sb-doped SnO_2 films was independently established from previous results of grazing incidence SAXS measurements.[11] The degree of asymmetry was determined as the ratio between the average radii of inertia R_z and R_y of the nanopores along the z and y directions perpendicular and parallel to the film surface, respectively. For undoped and 3% Sb-doped films fired at 650 °C, the ratios R_z/R_y were determined to be 1.5 and 2.2, respectively, thus indicating that Sb doping favors the formation of more elongated and oriented pores whose major axes are perpendicular to the external film surface. Thus, the SAXS results presented here indicate that the coarsening process is dominant in the plane perpendicular to the major axes of the nanopores.

TABLE I. Kinetic exponent α and α'/α ratio corresponding to undoped and Sb-doped SnO_2 films fired at different temperatures.

Sb doping (%)	Temperature (°C)	α	α'/α
0	450	−0.08±0.01	3.1±0.01
3	450	−0.10±0.01	3.0±0.01
0	650	−0.07±0.01	2.9±0.01
3	650	−0.09±0.01	2.1±0.01

We have plotted in Figs. 4(a) and 4(b) the scaled structure functions $F(x)$ for undoped and 3% Sb-doped samples fired for different periods of time at 650 °C using the function $I(q)q_1^d$, with $d=3$. The curves corresponding to the undoped film [Fig. 4(a)] clearly exhibit the scaling property while the same does not occur for the 3% Sb-doped film [Fig. 4(b)]. Nevertheless, we can notice that the scaling property for the 3% Sb-doped film is approximately obeyed if we consider the exponent $d=2$ instead of $d=3$ [Fig. 4(c)]. This is another (not independent) way that allowed us to establish that the coarsening in 3% Sb-doped samples fired at 650 °C is a two-dimensional process.

An independent way to demonstrate the bidimensional nature of the porous structure is through the analysis of the asymptotic behavior of $F(x)$ for $x>1$ that, as pointed out in Sec. II, are expected to be described by two power regimes. As can be seen in the double-logarithmic plots of our experimental results displayed in Fig. 5, corresponding to undoped

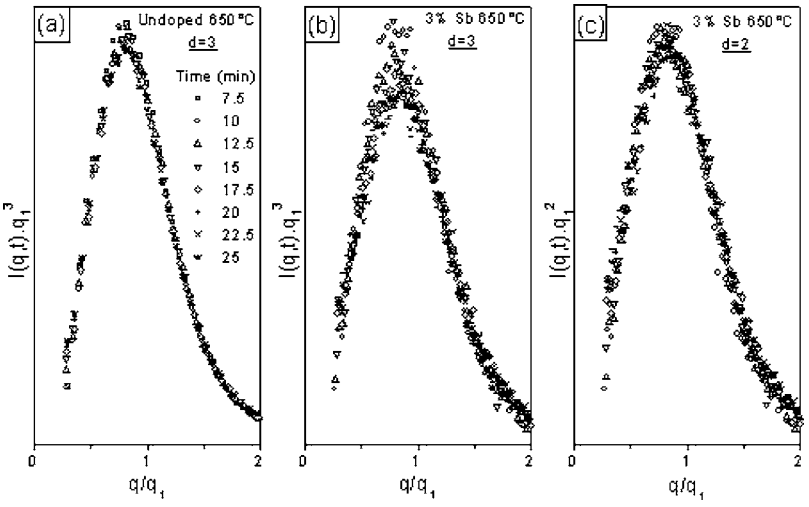

FIG. 4. Scaled structure functions (in arbitrary units) derived from SAXS curves measured at different time intervals at 650 °C. In (a) and (b), the scaled functions of undoped SnO_2 films and 3% Sb-doped films, respectively, are plotted as $F(x)=I(q,t)q_1^3$. In (c), the scaled function corresponding to 3% Sb-doped film is plotted as $F(x)=I(q,t)q_1^2$.

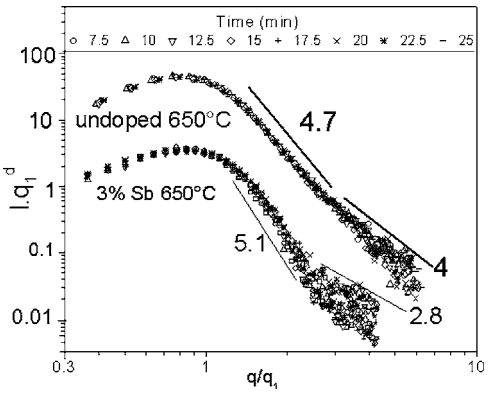

FIG. 5. Double-logarithmic plots of the scaled structure functions $F(x)=I(q,t)q_1^d$ (in arbitrary units) derived from the experimental SAXS curves corresponding to different time intervals at 650 °C for undoped ($d=3$) and 3% Sb-doped ($d=2$) SnO_2 films. The solid straight lines display the typical features predicted by the asymptotic behaviors specified by Eq. (2).

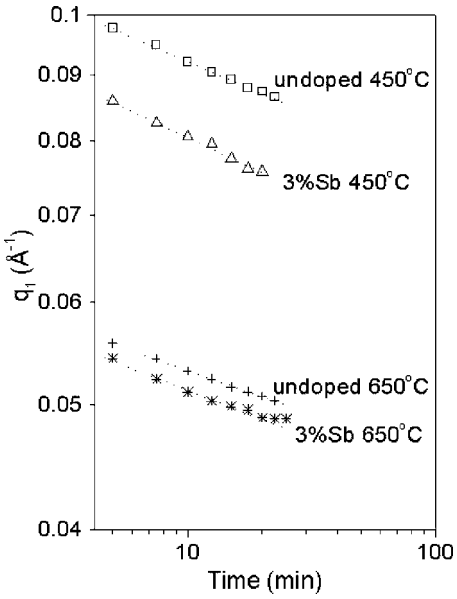

FIG. 6. Double-logarithmic plots of the normalized first moment q_1 as functions of the periods of time of isothermal treatment of undoped SnO_2 films and 3% Sb-doped SnO_2 films. Dotted lines represent linear least-squares fitting of Eq. (7).

and 3% Sb-doped samples fired for different periods of time at 650 °C, two linear regimes are observed for the scaled structure functions $F(x)$. At high reduced q values ($x>2.5$), the slope of the straight line in Fig. 5 for undoped samples is the expected for a power function $I(q)\propto x^p$ with $p\cong -4$ [Eq. (2)]. The exponent $p=-4$ determined from our experimental results implies that the Porod law is obeyed, this result indicating that (i) the pore-matrix interface is smooth and sharp and (ii) the film contains randomly oriented nanopores with an isotropic tridimensional structure ($d=-p-1=3$). On the other hand, for 3% Sb-doped samples, the asymptotic linear tail of $F(x)$ for $x>2.5$ corresponds to a power-law regime with an exponent $p=-2.8\pm0.3$, which suggests a quasi-two-dimensional coarsening process ($d=1.8\cong 2$). Furthermore, the steeper tail observed in Fig. 5 over an intermediate x range ($1<x<2.5$) with $|p|>4$, is a consequence of the topology of the interconnected pores framework. This feature has been interpreted in the percolated regime by the existence of a *wavy interface*.[28]

It should be stressed that the dynamical scaling property of anisotropic two-dimensional systems during coarsening processes has been reported by several authors and demonstrated by computer simulations performed under confined conditions, i.e., in very thin layers or in slab geometries with thicknesses similar to the values of the characteristic correlation distance $[R(t)=2\pi/q_1]$ in the plane.[31–35] Geometrical confinement effects were not expected in the samples studied here because the film thicknesses ($\approx$200 nm) are about ten times the largest $R(t)$ values derived from our SAXS curves. Therefore, the present study reveals the validity of the dynamic scaling hypothesis in intrinsic bidimensional coarsening processes. We expect that these experimental results will motivate further theoretical work in order to elucidate this somewhat unexpected finding.

B. Kinetic mechanism

The time variation of the normalized first moment $q_1(t)$ for undoped and Sb-doped films heat treated at 450 and 650 °C, are plotted in double-logarithmic scale in Fig. 6. The linear behavior predicted by Eq. (7) for the $\log q_1$ vs $\log t$ functions is clearly obeyed for all the systems studied here. As reported in Table I, the values of kinetic exponents α for undoped and 3% Sb-doped films are similar and do not change appreciably with the heat treatment temperature.

The value of kinetic exponent corresponding to the undoped SnO_2 supported film studied in this work ($\alpha\approx 0.09\pm0.01$) is lower than those reported in previous studies of unsupported SnO_2 thick film ($\alpha=0.14$)[16] and powdered SnO_2 xerogel ($\alpha=0.15$),[23] both studies done in a similar temperature range. The latter value is close to that theoretically predicted for solid cluster coagulation controlled by surface mobility in isotropic tridimensional systems,[28] while the value observed here ($\alpha\approx 0.09$) is not predicted by classical mechanisms of structure coarsening.

The rather low kinetic exponent ($\alpha\approx 0.09$) experimentally determined suggests that the grain growth process in supported films is hindered by the mechanical constraints imposed by the rigid substrate. In fact, it has been demonstrated in many experiments that large elastic misfits work against the grain coarsening in both ceramic and metallic binary alloys.[36,37] For example, a very low kinetic exponent, $\alpha\approx 0.09$, was determined for the coarsening process of a second phase in a perovskite-magnothowursite system.[36] This experimental observation is also supported by computer simulations. In particular, simulation results indicate that the elastic interactions between grains can decrease the kinetic exponent α down to very low values (say, 0.1 and lower) and can cause grain splitting, minimizing the elastic energy of the system.[38,39] This splitting phenomenon is controlled by the elastic to surface energy ratio.[39]

An interesting feature emerges from the comparison of the results corresponding to undoped films and 3% Sb-doped

films fired at 650 °C: in spite of the fact that the coarsening process of the former occurs in three dimensions and that of the latter in two dimensions, both exhibit essentially the same kinetic exponent. This suggests that the same transport mechanism controls the coarsening process for both undoped and 3% Sb-doped films. This finding is in agreement with modeling studies performed by computer simulation, suggesting that the value of kinetic exponent characteristic of isotropic coarsening is also expected for the growth of domains in highly anisotropic systems.[34,35]

However, the question that remains unclear is which factor is responsible for the change of the coarsening process from tridimensional to bidimensional by adding 3% of Sb in the undoped SnO_2 matrix. It is well known[28] that grain growth in solid systems is determined by the speed of the grain-boundary motion, which is proportional to the thermodynamic driving force for boundary migration F_b and to the boundary mobility M_b, the latter parameter depending on the kinetic-controlled transport mechanism. Similar values of the kinetic exponent α determined for undoped and 3% Sb-doped samples (Table I) suggest that the doping level does not significantly affect the grain-boundary mobility. It appears, therefore, that the 3% Sb doping affects F_b by decreasing the grain surface energy. Under the elastic stress imposed by the substrate, this effect may increase the elastic to surface energy ratio, thus favoring the grain splitting in the direction parallel to the substrate surface. As a consequence, for 3% Sb-doped films, coarsening occurs preferentially in the plane parallel to the substrate surface. This explanation, based on the decrease of the surface energy upon Sb doping, agrees with previous studies suggesting that Sb cations form a nonhomogeneous substitutional solid solution, replacing Sn atoms slightly below the grains surface.[18,40]

VI. CONCLUSION

In order to test the validity of the scaling and other statistical properties of the nanoporous structure of undoped SnO_2 and 3% Sb-doped SnO_2 thin films supported by a mica substrate during the coarsening process, we have measured *in situ* several series of SAXS scattering curves for different periods of time at 450 and 650 °C. By comparing experimental SAXS results and theoretical predictions, we have clearly established the validity of the scaling property and determined the effects of Sb doping on the dimensionality of the coarsening process occurring in these sol-gel dip-coated films.

From the analysis of the experimental results, we have concluded that in undoped and 3% Sb-doped films fired at 450 °C, the volume fraction of nanopores decreases during the first 10–15 min of isothermal treatment, this feature being a consequence of the total nanopore volume variation produced by secondary condensation reactions involving OH groups present at the particle boundaries. For undoped films fired at 650 °C, this condensation effect is very fast and could not be detected in our time-resolved SAXS experiments.

For undoped samples fired at 650 °C, the experimental structure function $S(q,t)$ exhibits the dynamical scaling properties expected for isotropic structure and tridimensional coarsening process, while for 3% Sb-doped films also fired at 650 °C, clear deviations from this behavior were observed. The experimental structure function of 3% Sb-doped films fired at 650 °C also exhibit the dynamical scaling properties if the coarsening process is assumed to be in two dimensions instead of three.

The value of the kinetic exponent for the coarsening process, α, for undoped SnO_2 supported film studied here ($\alpha \approx 0.09 \pm 0.01$) is lower than those reported in previous studies over a similar temperature range of unsupported nondoped SnO_2 thick films ($\alpha=0.14$) and powdered SnO_2 xerogels ($\alpha=0.15$). This finding evidences that the grain and pore coarsening process in supported films is hindered by mechanical constraints imposed by the rigid substrate.

ACKNOWLEDGMENTS

We acknowledge the LNLS staff for SAXS measurements and the Brazilian agencies CAPES, CNPq, and FAPESP for financial support.

*Email address: santilli@iq.unesp.br

[1] S. J. Blunden, P. A. Cusak, and R. Hill, *The Industrial Uses of Tin Chemicals* (Royal Society of Chemistry, London, 1985).
[2] U. Zum Felde, M. Haase, and H. Weller, J. Phys. Chem. B **104**, 9388 (2000).
[3] T. Nutz, U. Zum Felde, and M. Haase, J. Chem. Phys. **110**, 12142 (1999).
[4] V. Dusastre and D. E. Williams, J. Phys. Chem. B **102**, 6732 (1998).
[5] G. Boschloo and D. Fitzmaurice, J. Phys. Chem. B **103**, 3093 (1999).
[6] C. Terriera, J. P. Chatelona, R. Berjoanb, and J. A. Rogera, Thin Solid Films **263**, 37 (1995).
[7] S. S. Park and J. D. Mackenzie, J. Am. Ceram. Soc. **78**, 2669 (1995).
[8] A. E. De Souza, S. H. Monteiro, C. V. Santilli, and S. H. Pulcinelli, J. Mater. Sci.: Mater. Electron. **8**, 267 (1997).
[9] M. A. Aegerter, A. Reich, D. Ganz, G. Gasparro, J. Piitz, and T. Krajewski, J. Non-Cryst. Solids **218**, 123 (1997).
[10] G. Gasparro, J. Putz, D. Ganz, and M. A. Aegerter, Sol. Energy Mater. Sol. Cells **54**, 287 (1998).
[11] A. P. Rizzato, C. V. Santilli, S. H. Pulcinelli, and A. F. Craievich, J. Appl. Crystallogr. **36**, 736 (2003).
[12] E. R. Leite, M. I. B. Bernardi, E. Longo, J. A. Varela, and C. A. Paskocimas, Thin Solid Films **449**, 67 (2004).
[13] Y. Hu and S. H. Hou, Mater. Chem. Phys. **86**, 21 (2004).
[14] V. Geraldo, L. V. A. Scalvi, E. A. Morais, C. V. Santilli, P. B. Miranda, and T. J. Pereira, J. Eur. Ceram. Soc. **25**, 2825 (2005).
[15] V. Briois, C. V. Santilli, and S. H. Pulcinelli, J. Mater. Sci. Lett. **20**, 555 (2001).

[16] G. E. S. Brito, C. V. Santilli, S. H. Pulcinelli, and A. F. Craievich, J. Non-Cryst. Solids **217**, 41 (1997).
[17] C. V. Santilli, S. H. Pulcinelli, G. E. S. Brito, and V. Briois, J. Phys. Chem. B **103**, 2660 (1999).
[18] J. Rockenberger, U. Zum Felde, M. Tischer, L. Troger, M. Haaseb, and H. Weller, J. Chem. Phys. **112**, 4296 (2000).
[19] F. Montilla, E. Morallón, A. De Battisti, S. Barison, S. Daolio, and J. L. Vázquez, J. Phys. Chem. B **108**, 15976 (2004).
[20] C. McGinley, H. Borchert, M. Pflughoefft, S. Al Moussalami, A. R. B. de Castro, M. Haase, H. Weller, and T. Möller, Phys. Rev. B **64**, 245312 (2001).
[21] B. Grzeta, E. Tkalcec, C. Goebbert, M. Taked, M. Takhashi, K. Nomura, and M. Jaksic, J. Phys. Chem. Solids **63**, 765 (2002).
[22] B. Orel, U. Lavrencic-Stangar, Z. Crnjak-Orel, P. Bukovec, and M. Kosec, J. Non-Cryst. Solids **167**, 272 (1994).
[23] C. V. Santilli, S. H. Pulcinelli, and A. F. Craievich, Phys. Rev. B **51**, 8801 (1995).
[24] J. Marro, J. L. Lebowitz, and M. H. Kalos, Phys. Rev. Lett. **43**, 282 (1979).
[25] K. Binder, Phys. Rev. B **15**, 4425 (1977).
[26] H. Furukawa, Phys. Rev. A **23**, 1535 (1981).
[27] H. D. Bale and P. W. Schmidt, Phys. Rev. Lett. **53**, 596 (1984).
[28] H. Furukawa, J. Appl. Crystallogr. **21**, 805 (1988).
[29] A. P. Rizzato, C. V. Santilli, and S. H. Pulcinelli, J. Sol-Gel Sci. Technol. **19**, 811 (2000).
[30] G. E. S. Brito, S. H. Pulcinelli, and C. V. Santilli, J. Mater. Sci. **31**, 4087 (1996).
[31] A. P. Y. Wong, P. Wiltzius, and B. Yurke, Phys. Rev. Lett. **68**, 3583 (1992).
[32] B. D. Butler, H. J. M. Hanley, D. Hansen, and D. J. Evans, Phys. Rev. B **53**, 2450 (1996).
[33] O. M. Braun, M. V. Paliy, and M. Peyrard, Phys. Rev. B **55**, 4797 (1997).
[34] M.-Carmen Miguel and R. Pastor-Satorras, Phys. Rev. E **59**, 826 (1999).
[35] F. Lallet, R. Bachelet, A. Dauger, and N. Olivi-Tran, Phys. Rev. B **74**, 075411 (2006).
[36] D. Yamazaki, T. Kato, E. Ohtani, and M. Toriumi, Science **274**, 2052 (1996).
[37] J. W. Martin and F. J Humphareys, Scr. Metall. **8**, 679 (1974).
[38] H. Nishimori and A. Onuki, Phys. Rev. B **42**, 980 (1990).
[39] P. W. Voorhees, Annu. Rev. Mater. Sci. **22**, 197 (1992).
[40] B. Slater, C. Richard, A. Catlow, D. H. Gay, D. E. Williams, and V. Dusastre, J. Phys. Chem. B **103**, 10644 (1999).